Internet of Things 7 (2019) 100082

Contents lists available at ScienceDirect

Internet of Things

journal homepage: www.elsevier.com/locate/iot

Research article

# Self-sustainable power-collecting node in IoT

John Anzola [a,b,*], Andrés Jiménez [a], Giovanny Tarazona [b]

[a] Engineer Faculty, Department of Electronics and Systems, Fundación Universitaria Los Libertadores, Carrera 16 #63A-68, Bogotá, D.C., Colombia

[b] Doctorate in Engineering, Universidad Distrital Francisco José de Caldas, Carrera 7 No. 40B-53, Bogotá, D.C., Colombia

ARTICLE INFO

*Article history:*
Received 28 April 2019
Revised 1 July 2019
Accepted 3 July 2019
Available online 5 July 2019

*Keywords:*
Wireless sensor networks
IoT
Ni-MH batteries
Energy harvesting

ABSTRACT

This article details the energy analysis of a sustainable node in time (NodeMCU), using a solar energy collection system with NiMh backup batteries during the night, rainy days, and low solar brightness days. The solar power collection system was characterized by extracting data from Sunny, Cloudy, and Rainy days from the AccuWeather weather information system, as the Colombian Institute of Hydrology, Meteorology and Environmental Studies only provides monthly information. The system was implemented using a very low-speed TDMA data transmission scheme, which used 8 GET HTTP requests to transmit the following information: The first field is the input voltage of the node power regulator, and the remaining fields the value is zero, filling a complete time slot. This information was transmitted to the ThingSpeak platform, which registered the behavior of the solar power collection system over a period six months, monitoring the stability, autonomy, and sustainability of the node.

© 2019 Elsevier B.V. All rights reserved.

## 1. Introduction

A wireless sensor network (WSN) is a wireless network that contains nodes or devices distributed in space. Each node is comprised of a transceiver and a processing unit, usually a microcontroller that allows connecting sensors and, optionally, actuators. These nodes require an energy system for power. The basic function of the nodes is data collection from their environment through a sensor system for different applications [1–3]. This data is transmitted over a wireless network by means of multi-hop or hierarchical communication schemes, depending on the coverage area and the topological distribution of the nodes in space.

One of the hierarchical approaches to WSNs involves sending data to a central node (receiving node). If the central node is within range, the topology generated is a star topology with a distance of one hop. However, given the high density of nodes, a networked power management system is usually required, either by software, hardware or mixed. One of the software solutions is the use of MAC (media access control), which is challenge-based and may result in internal interference due to packet collision, causing greater energy usage due to lost packets being retransmitted. Another software solution is

*Abbreviations:* IoT, Internet of Things; NiMh, Nickel-Metal Hydride; TDMA, Time-Division Multiple Access; HTTP, Hypertext Transfer Protocol; WSN, Wireless Sensor Network; MAC, Media Access Control; API, Application Programming Interface; RF, Radio Frequency; GSM, Global System for Mobile communications; AM, Amplitude Modulation; NiCd, Nickel-Cadmium; Li-ion, Lithium-Ion; Li-Poly, Lithium Polymer; LDO, Low-Dropout; SoC, System on Chip; RAM, Random-Access Memory; ADC, Analog-to-Digital Converter; GPIO, General Purpose Input Output.

* Corresponding author at: Engineer Faculty, Department of Electronics and Systems, Fundación Universitaria Los Libertadores, Carrera 16 #63A-68, Bogotá, D.C., Colombia.

*E-mail addresses:* jpanzolaa@libertadores.edu.co (J. Anzola), acjimeneza@libertadores.edu.co (A. Jiménez), gtarazona@udistrital.edu.co (G. Tarazona).

https://doi.org/10.1016/j.iot.2019.100082
2542-6605/© 2019 Elsevier B.V. All rights reserved.

**Table 1**
Energy collection systems power density.

| Energy sources | Power density | Harvesting methods |
|---|---|---|
| Solar (outdoors) | 100 mW/cm$^3$ | Solar cells |
| Solar (indoors) | 100 μW/cm$^3$ | Indoor solar cells |
| Vibrations (human motion) | 4 μW/cm$^3$ | Piezoelectric/Electrostatic |
| Vibrations (machine motion) | 800 μW/cm$^3$ | Electromagnetic |
| Wind | 177 μW/cm$^3$ | Generator |
| Thermal (human) | 60 μW/cm$^3$ | Thermal electric |
| Thermal (industry) | 10 mW/cm$^3$ | Thermal electric |
| Radio frequency (RF-GSM) | 300 μW/cm$^3$ | Patch antenna |
| Radio frequency (RF-WiFi) | 150 μW/cm$^3$ | Magnetic coil antenna |
| Radio frequency (RF-AM) | 2 mW/cm$^3$ | Magnetic coil antenna |

based on TDMA (time division multiple access), which avoids internal interference by sacrificing data rate and power usage compared to the MAC protocol. TDMA divides the time into fixed time slots, guaranteeing sufficient time to transmit a single packet and receive confirmation.

Several approaches have been proposed for WSNs using MAC, TDMA, and their derivatives, structured and unstructured, for data collection and aggregation, resulting in different grouping and routing protocols aimed and preserving and improving network life span [4,5].

Hardware-based solutions focus on the physical level of nodes, proposing polling strategies for sensor readouts, real-time operating system algorithms [6,7], focus on sleep scheduling [8], antennas [9], and others, all concerned with energy savings through hardware and software node modifications.

Energy source approaches have faced energy sustainability challenges, due to the need to integrate several power supplies in each node to extend its life span in the network. In a WSN, power collectors provide a small amount of energy for low-power nodes. High-power elements require fuel to generate power, which increases the cost. Power collector approaches exploit sustainable power generation technologies to substitute carbon, oil and natural gas-based energy sources, as their emissions damage the environment.

There are millions of nodes and devices capable of working with rechargeable (which require recharge cycles) and non-rechargeable batteries (of limited durability.) In high-density network configurations, these batteries require either replacement or demand access to alternate power outlets and wiring, and the setup of battery chargers. In case of using non-rechargeable batteries, nodes require the periodic replacement of batteries.

To solve these power collection issues, the present article focuses on the design of a low-cost node based on the NodeMCU card, which reads the voltage value of the battery and packages it in the field 1 of 8, through a GET HTTP request from the ThingSpeak API. The rest of the fields are transmitted with a value of zero, fillning the 8 GET HTTP requests in a time slot, which are transmitted through TDMA. The node's power source is based on a rechargeable Nickel-Metal Hydride battery connected to a generic 10W 5V output solar cell. Its energy behavior was analyzed over a 6-month period, proving its sustainability over time. The proposed design also matches the characteristics of ThingSpeak's API, with a minimum data storage frequency that qualifies for the Home license, which is reserved for personal use only.

## 2. Work performed

### *2.1. Energy collection systems for a WSN*

The report "Global Markets, Technologies, and Devices for Energy Harvesting," presents a forecast about energy collectors being used to power WSNs in the future, partly due to the growth of Internet of Things technologies (IoT) [10,11]. This report estimates that energy collectors will power devices that will not be as prolific as wireless nodes, for applications using piezoelectric power collection [12], vibration [13], thermal-electric [14], RF-energy [15] and solar [16].

Table 1 shows some energy collection systems used to power WSN nodes, compared by power density [17].

As shown in Table 1, solar power collection provides higher power density and is the most used of all energy collection systems to power WSN nodes. For this reason, it was selected as the energy collection source to design the node proposed in this article.

### *2.2. Battery types for energy storage*

One of the most important elements in an energy collection system is the power storage system, which can use rechargeable batteries or supercapacitors. Supercapacitors work similarly to conventional electrolytic condensers, with the difference that supercapacitors work in the Faradaic capacitance range [18].

One of the main advantages of supercapacitors as compared to batteries is their its ability provide power. Supercapacitors are capable of supplying more power than batteries, albeit with a lower energy density. Another disadvantage of supercapacitors is leakage current, which increases proportionality to their capacitance value [19].

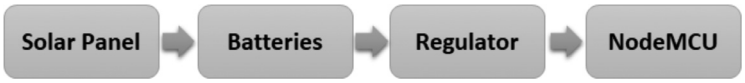


**Fig. 1.** Block diagram of the solar power collection system.

**Table 2**
Rechargeable batteries properties [20].

| Properties | NiCd | NiMH | Li-ion | Li-Poly |
|---|---|---|---|---|
| Gravimetric Energy Density (Wh/kg) | 45 to 80 | 60 to 120 | 110 to 160 | 100 to 130 |
| Cycle Life (to 80% of initial capacity) | 1500 | 300 to 500 | 500 to 1000 | 300 to 500 |
| Self-discharge/Month (room temperature) | 20% | 30% | 10% | 10% |
| Rated voltage (V) | 1.25 | 1.24 | 3.6 | 2.7 |

**Table 3**
Specification of solar panel module.

| Parameters | Value |
|---|---|
| Module Types | 10 Watt Monocrystalline |
| Maximum power (Pmp) | 10 Wp |
| Open Circuit Voltage (Voc) | 6.8 V |
| Maximum Power Voltage | 5 V |
| Maximum Power Current | 1200 mA |
| Short Circuit Current (Isc) | 1700 mA |
| Series Fuse | Class C |

The solar power collection energy storage system proposed used NiMH batteries, due to their high capacity and energy density. Table 2 shows a comparison between generic rechargeable batteries.

The life span of a battery is defined as the number of charge cycles. NiMh and LiPoly batteries, as shown in Table 2, have a life span of 300 to 500 charge cycles. Once the limit is reached, batteries usually lose 20% of capacity, which results in a shorter duration of charge.

NiCd batteries self discharge at a rate of 10% in the first 24 hours and an additional 10% over 30 days. In this sense, NiMH batteries have the highest levels of self-discharge.

## 3. Solar power collection system design

The solar power collection system proposed in this article aims to achieve energy sustainability for a node based on NodeMCU. The overall design includes four components: solar panel, Ni-MH batteries, voltage regulator, and the NodeMCU, as shown in Fig. 1.

### *3.1. Solar panel*

In the selection of a solar panel for the energy collection system design, the first considerations were the power consumption of the node and the battery charge capacity.

After determining the power of the device without any power saving strategies (no sleep mode), a solar panel was selected according to the voltage requirements of the open circuit and short circuit current, based on the I-V curve, which determined that the power output of the panel was sufficient to provide the required energy to charge the batteries and power the node. Table 3 shows the solar panel characteristics.

### *3.2. Power storage*

Power storage is one of the fundamental components of a solar power collection system, as it comprises methods to preserve energy for its usage on-demand. Table 2 shows the most common generic battery types, with the following characteristics: Nickel Cadmium batteries (NiCd) have the highest discharge rate. Cadmium batteries are highly polluting and were ruled out in the design phase.

Nickel-Metal Hydride (Ni-MH) batteries have a higher energy storage capacity than Lithium-Ion batteries (Li-Ion). Ni-MH batteries can be trickle-charged by a low-current input. Li-Ion batteries are more efficient in their discharge and recharge cycles and have higher energy density than Ni-MH batteries [21]. However, Li-Ion batteries are more expensive and require additional electronic circuitry to maintain charge and recharge conditions, protection, and to extend battery life. The use of an additional circuit rules out the use of Li-Ion batteries, as the desired design was intended to be both low-cost and

**Table 4**
Features AMS1117.

| Parameters | Value |
|---|---|
| Three Terminal Adjustable or Fixed Voltages | 1.5 V, 1.8 V, 2.5 V, 2.8 5V, 3.3 V and 5.0 V |
| Output Current | 800 mA |
| Minimum Load Current | 5 mA |
| Voltage dropout | 1.3 V |
| Line Regulation | ±0.2% |
| Maximum input voltage | 12 V |

minimalistic. Lithium Polymer (Li-Po) batteries derived from Li-Ion batteries were also ruled out due to their higher cost. Ni-MH batteries were chosen as they are the least expensive in the Colombian market and are easy to acquire. The proposed design uses Energizer NM15 reference Ni-MH batteries.

### 3.3. Low drop out line regulator

The NodeMCU node includes an integrated Low dropout (LDO) linear regulator AMS1117 configured at 3.3 V, which is able to regulate an input voltage range from 4.0 to 12 V, with a 3.3 V, 800 mA fixed output voltage [22]. LDO regulators transfer more energy to charge, minimizing energy losses, as the tension drop between its input and output terminals is considerably low, compared to conventional or bipolar regulators. The NodeMCU node uses power dissipation through its printed circuit to deliver a quiescent current of 5 mA to 11 mA, reaching operational currents of about 80 mA. Table 4 shows the regulator characteristics.

### 3.4. NodeMCU node

The NodeMCU node is a development board that integrates the SoC ESP8266, designed and manufactured by Espressif Systems. This board includes a 32-bit, low-power microcontroller (Tensilica L106), a 2.4 GHz WiFi module, 50 kB of RAM memory, an analog-to-digital converter (ADC) and 17 input and output general purpose pins (GPIO). Due to its low cost, the NodeMCU node is one of the best platforms for IoT application development. It includes an event-controlled API for network applications, which simplifies the development process.

## 4. Methodology

General description of the design considerations of the solar power collection system. Firstly, experimental tests were conducted in the Soacha Cundinamarca town, located 21 Km away from Bogotá, D.C., Colombia (Latitude: 4.581304; Longitude: −74.214999; Altitude: 2561 meters). To establish the characteristics of the I-V curve and the integration of the solar panel with the NodeMCU node, power usage calculations of the NodeMCU node were performed, along with the power calculations with battery supply and the calculation of proportional energy delivered by the solar panel, integrating the general design considerations of the node.

### 4.1. Energy usage of NodeMCU

Based on the NodeMCU datasheet, the average power usage in active mode (active microcontroller + transceiver) is 80 mA [23]. This value was confirmed in experimental testing by using the tension drop value in a resistance with a nominal value of 1Ω and a real measured value of 0.987Ω ± 5%. This resistance was connected in series to the power supply and the NodeMCU node (see Fig. 2).

Once the operating current value was determined, and considering that the LDO regulator voltage for NodeMCU is of 3.3 V, the power ($P$) was calculated as shown in Eq. (1).

$$P = V \times I$$
$$P = 3.3\,\mathrm{V} \times 80\,\mathrm{mA} = 264\,\mathrm{mW} \tag{1}$$

Eq. (2) calculates the energy ($E$) usage of the NodeMCU node for a day.

$$E = V \times I \times t$$
$$E = 3.3\,\mathrm{V} \times 80\,\mathrm{mA} \times 24 \times 3600\,s = 22809.6\,\mathrm{J} \tag{2}$$

### 4.2. Energy calculation of the batteries

Eq. (3), calculates the energy provided by the 1300 mAh Ni-MH batteries, with a nominal voltage of 3.75 V. The total energy ($B$) supplied by the batteries is:

$$B = 3.75\,\mathrm{V} \times 1300\,\mathrm{mA} \times 60 \times 60\,\mathrm{s} = 17550\,\mathrm{J} \tag{3}$$

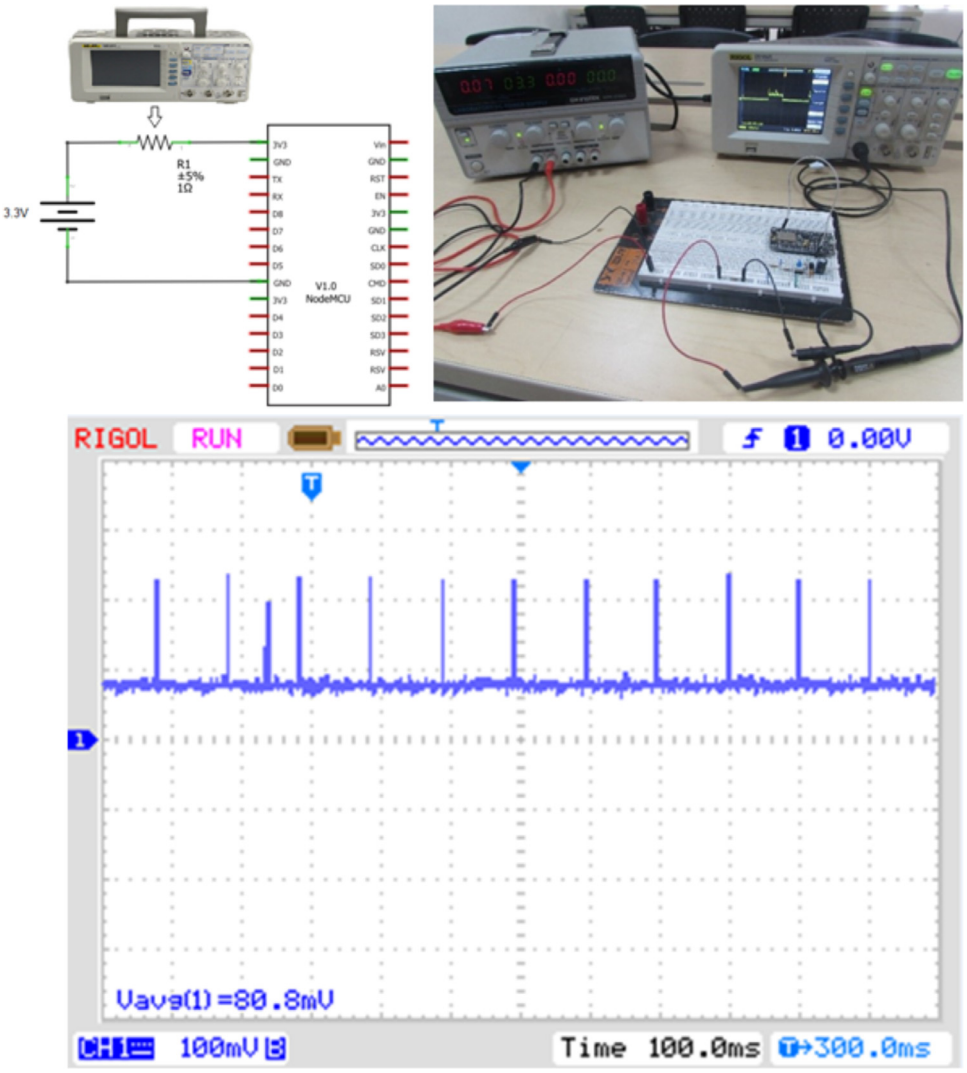


**Fig. 2.** Operating current of the NodeMCU node.

**Table 5**
Averages of current and voltage of the solar panel in different weather conditions.

| State | Hours | Average Current (mA) | Average output voltage (V) |
|---|---|---|---|
| Sunny | 96.6 | 200 | 4.96 |
| Cloudy | 248.5 | 122 | 4.74 |
| Rainy | 14.9 | 67 | 4.1 |

Eq. (4) calculates the energy supply time ($T_b$) of the batteries:

$$T_b = \frac{B}{E} = \frac{17550}{22809.6} = 0.76\,\text{days} \tag{4}$$

### 4.3. Energy supply calculation of the solar panel

To calculate the energy provided by the solar panel, three climate conditions were considered: cloudy, sunny, and rainy. For these three conditions, tests in the Soacha Cundinamarca town were performed for 30 of June, taking the daily data from 6:00 am to 6:00 pm. The average current and voltage data are shown in Table 5. The classification of sunny, cloudy, and rainy was extracted from the website AccuWeather [24] through the use of a Python script that extracts the values contained in the tag span class=“cond” as shown in Fig. 3, and its value was classified under the conditions shown in Fig. 4.

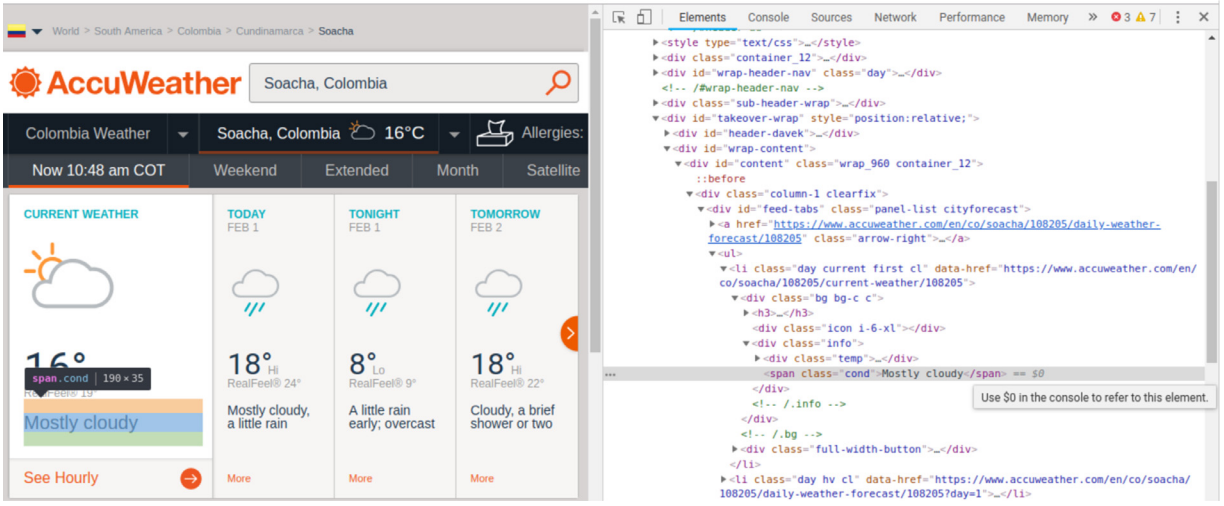


**Fig. 3.** Extraction of state.

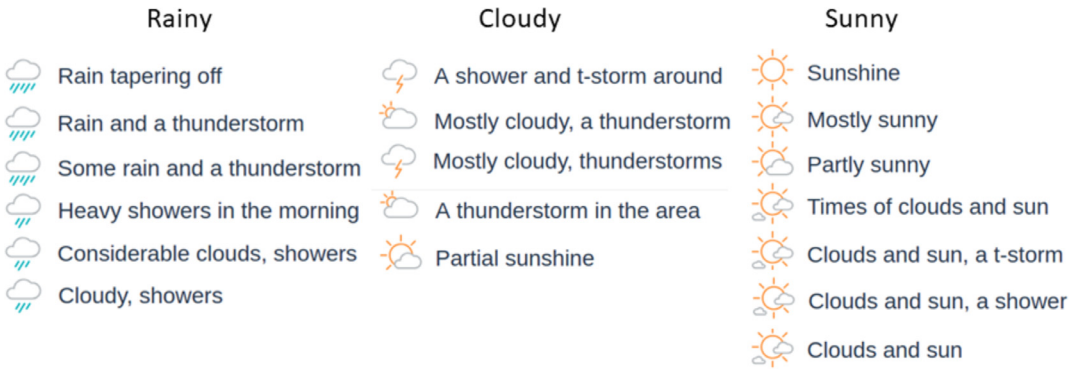


**Fig. 4.** Status classification.

Below is the energy calculation ($S$) with the day where the least amount of sunlight and the highest amount of rain for the collection system. The LDO regulator output shows an operating voltage of 3.3 V, as the regulator input value is higher than 3.3 V. The energy calculation was obtained through Eq. (5) with the least favorable condition, as it was cloudy for 8 h, rainy for 3 h, and sunny for 1 h.

$$S = 3.3\,\mathrm{V} \times (0.2A \times 1\,\mathrm{h} + 0.122A \times 8\,\mathrm{h} + 0.067\,\mathrm{A} \times 3\,\mathrm{h}) \times 3600\,\mathrm{s}$$
$$S = 16358.76\,\mathrm{J} \tag{5}$$

Eq. (6), calculates the time required by the energy collection system ($T_C$) to charge the batteries fully.

$$T_C = \frac{B}{S} = \frac{17550}{16358.76} = 1.072\,\mathrm{days} \tag{6}$$

At this point, the solar panel requires 1.072 days to charge the batteries fully. This condition was obtained through the transmission of 8 messages. The first message compiles the battery voltage value in the first field, with the following 7 fields all including zero values. Messages were transmitted through a GET HTTP request using ThingSpeak's API. The 8 messages were transmitted in a single time slot of a TDMA data transmission scheme. In the tests, each time slot is 30 seconds long, during which the transmission of each message takes less than 1 second. In the tests, the node remained in an active state, and normal operational current is 80 mA. Under the aforementioned tests and conditions, the batteries are capable of powering the node for 0.76 days (see Eq. (4)).

The 30-second time slot was selected to make the proposed system compatible with the IoT platforms shown in Table 6. These platforms operate under a personal usage license and without costs under certain restrictions and limitations. The ThingSpeak API was selected due to its annual storage. It has three channels, where each of the channels includes 8 fields to store 8 variables. This API is widely used in the IoT industry.

For the time slot, the strategy used required using the node in sleep mode for a 20-second interval to save energy. For the following 10 to 12 seconds in the time slot, the node switched from sleep to active mode, connected to the Internet

**Table 6**
IoT Platforms.

| Platform | Number of channels | Persistent messages (day/year) | Data retention |
|---|---|---|---|
| Beebotte | Unlimited | 5000/day | 3 months |
| Iothook | 3 | 4300/day | 1 month |
| DataGekko | Unlimited | 1440/day | 7 days |
| IoTPlotter | 1 | 5760/day | 1 month |
| Horavue | 10 | 1 GB/year | 1 year |
| ThingSpeak | 8 | 8200/day | 1 year |

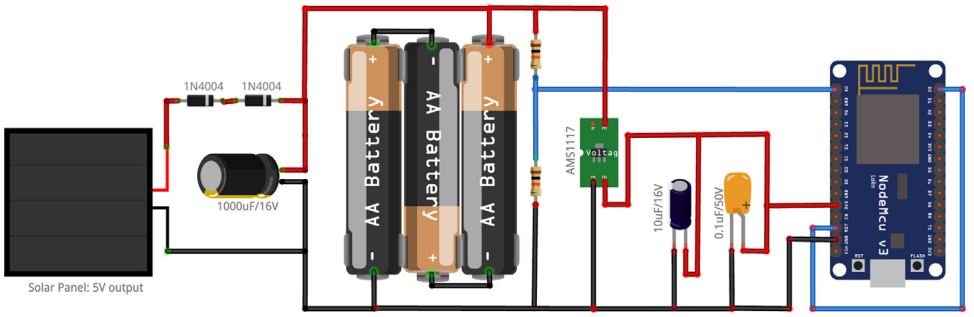


**Fig. 5.** Schematics for the solar power collection system.

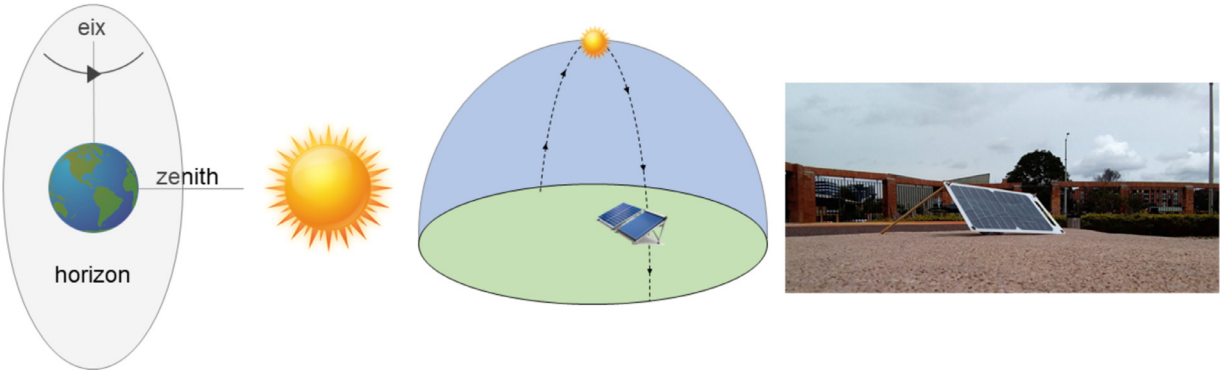


**Fig. 6.** Experimental configuration for the solar energy collection circuit.

and transmitted 8 messages. For the first message, the battery voltage readout was converted from analog to digital. The following 7 messages were zeroed out, leaving the option to transmit additional sensor values in the future. Eq. (7) calculates the work cycle ($D$) in which the node remains active in a time slot.

$$D = \frac{Active\,time}{Active\,time + Sleep\,time} \times 100\% = \frac{12s}{12s + 20s} \times 100\% = 37.5\% \tag{7}$$

For a 37.5% work cycle with 80 mA in active mode (active microcontroller + transceiver), and power usage of 10 uA in sleep mode, the mean power usage of the system is 30 mA. Eq. (8) shows the working power for this power cycle.

$$P = 3.3\,\mathrm{V} \times 30\,\mathrm{mA} = 99\,\mathrm{mW} \tag{8}$$

Eq. (9) calculates the energy ($E$) used by the node in a 37.5% work cycle over a single day.

$$E = 99\,\mathrm{mW} \times 24\,h \times 3600\,\mathrm{s} = 8553.6\,\mathrm{J} \tag{9}$$

Eq. (10) calculates the battery energy supply time ($T_b$) to the node in a 37.5% work cycle.

$$T_b = \frac{B}{E} = \frac{17550}{8553.6} = 2.05\,\mathrm{days} \tag{10}$$

Eq. (6) estimates a time of 1.072 days for the energy collection system to recharge the batteries fully. With a sleep mode activation resulting in a 37.5% work cycle, the result is a 2-day autonomy to power the node without the energy collection system. At this point, the equation calculates that the energy system is self-sustainable. Figs. 5 and 6 show the schematic and physical diagrams using the solar power collection system.

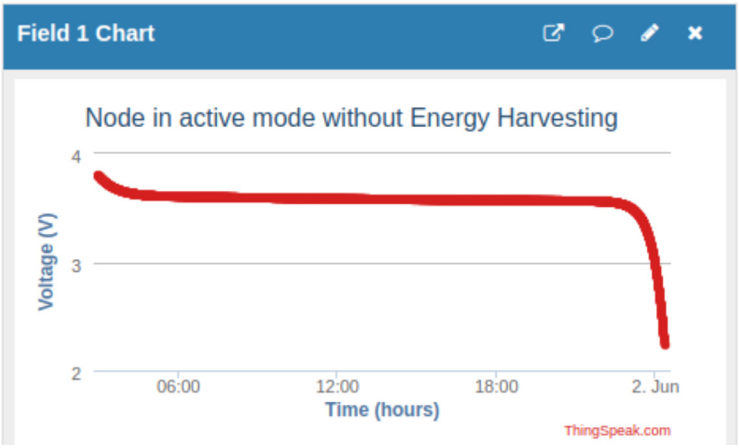


**Fig. 7.** The node in active mode, without a solar power collection system.

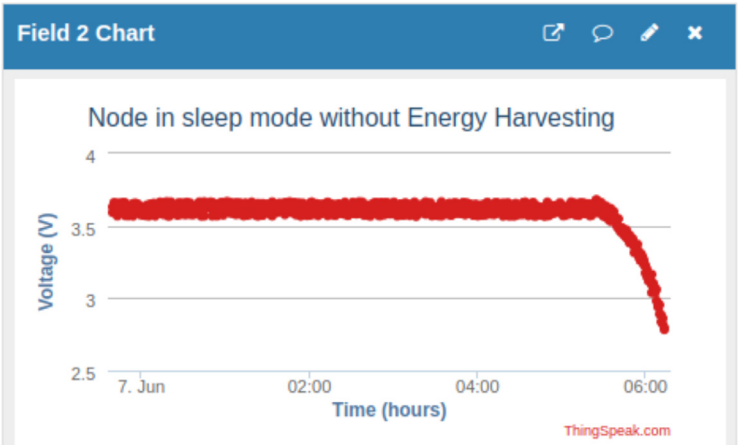


**Fig. 8.** Node in sleep mode without Solar Energy Harvesting.

## 5. Results analysis

### *5.1. Working results of the solar energy collection system*

The initial tests lasted 30 days in the month of June, allowing to observe the performance of the node in active mode and sleep mode for a 37.5% work cycle, with the aim of analyzing the power supply of the batteries, without the solar panel. Then, the solar power collection system was analyzed with the sleep mode activated for a 37.5% work cycle, with partial results of energy sustainability, which were then further assessed through the months of July to December.

In the initial tests, it was observed that the battery energy supply to the node without a solar panel was of 0.76, which is equivalent to 18.2 h. This result was obtained in active mode, in which 18.2 h resulted in a discharge of the batteries from 3.75 V to 3.2 V, which rendered the node unstable. 10 battery discharge tests were performed, with a resulting time range of 17.92 to 18.35 h, with an average of 18.124 and a variance of 0.018248, as shown in Fig. 7.

The battery energy supply time to the node in sleep time with a for a 37.5% work cycle, without the solar power collection system, had an estimated value of 2 days, as shown in Fig. 8. Experimental values ranged between 1.66 and 2.17 days over 10 tests, with an average of 1.923 days and a variance of 0.0187.

The solar power collection system was implemented with a node in sleep mode with a 37.5% work cycle, which resulted in a battery recharge time of 1.072 days (see Eq. (6)), equivalent to 25.848 hours. It is of note that the geographical location of Colombia, as it is located between the tropics, it keeps an average of hours of sunlight through the year. The batteries were charged up to 65.71% during daylight time. During the nighttime, the node batteries were discharged 16.42%, reaching full battery charge of 100% during the following day, in a total of about 35 h, as shown in Fig. 9.

Partial energy sustainability results for three days are shown in Fig. 10.

The solar power collection system sustainability was evaluated during the months of July to December, with the support of average solar irradiation levels for the town of Soacha. The data were obtained from the interactive solar atlas of the

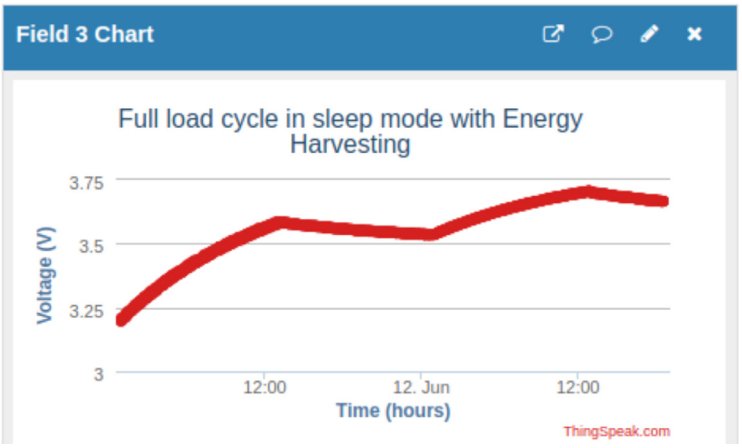


**Fig. 9.** Full battery charge cycle for the node in sleep mode with a 37.5% work cycle using the solar power collection system.

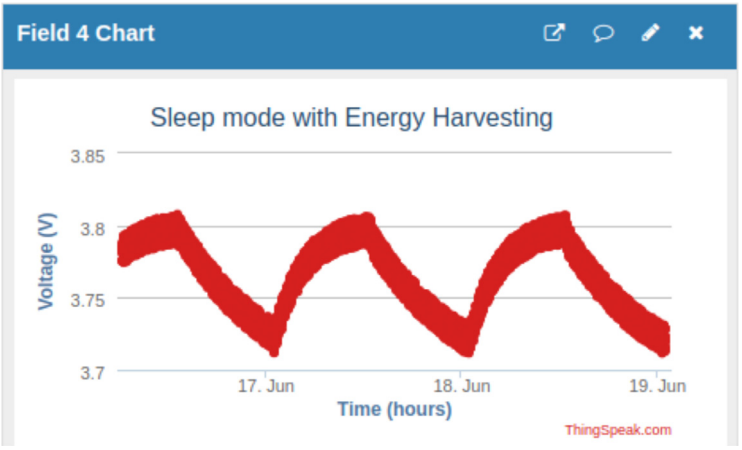


**Fig. 10.** Battery charge and discharge using the energy collection system for the first 3 days.

Institute of Hydrology, Meteorology and Environmental Studies [25], obtaining an average monthly irradiation value in $Wh/m^2$ as shown in Table 7 and a comparison with the solar brightness duration in hours, as key factor that enabled the analysis of the direct sunlight incidence over the solar panel and its direct proportion relationship with the monthly average voltage produced by the energy collection system, as shown in Fig. 11.

At this point, three variables were determined: irradiation ($Wh/m^2$), sunshine, and voltage provided by the solar panel to the NodeMCU node. Table 8 shows the average values of these three variables.

To determine the statistical validity of the results presented, we will first apply a covariance matrix with values shown in Table 9, depicting the degree of joint variation of the variables irradiation, sunshine, and voltage as compared to their average values. The output data of this matrix will allow determining the existence of dependence between the variables on a qualitative basis. Then, we will use the Pearson correlation Matrix (see Table 10) to estimate the degree of the linear relationship between the variables by estimating the strength of the relationship between them.

The values in the covariance matrix shown in Table 9 are positive, thus indicating that the above average values of the variables are associated. Unlike the data in the correlation matrix, the covariance values are not standardized, so the results obtained indicate a qualitative relationship of direct proportion between the irradiation, sunshine, and voltage variables. In this sense, the duration of sunshine (measured in hours) represents the total time in which direct sunlight strikes the surface of the solar panel between dawn and dusk. The results of the covariance matrix suggest that a greater sunshine value results in greater solar irradiation and a higher voltage produced by the solar panel, and vice versa.

The values of the correlation matrix in Table 10 show that the correlation values between variables are positive and are reflected in the direction, as the values in the covariance matrix tend to increase or decrease simultaneously, as the correlation metric is derived from the covariance. The values of the correlation matrix allow estimating the strength (correlation values close to 1) between the variables.

**Table 7**
Average radiation schedule (W/m$^2$).

| Hour | Jul | Aug | Sep | Oct | Nov | Dec |
|---|---|---|---|---|---|---|
| 0-1 | 0.3 | 0.4 | 0.5 | 0.2 | 0.3 | 0.3 |
| 1-2 | 0.4 | 0.5 | 0.4 | 0.2 | 0.4 | 0.4 |
| 2-3 | 0.5 | 0.5 | 0.4 | 0.2 | 0.3 | 0.3 |
| 3-4 | 0.3 | 0.4 | 0.5 | 0.2 | 0.3 | 0.3 |
| 4-5 | 0.3 | 0.4 | 0.5 | 0.2 | 0.4 | 0.3 |
| 5-6 | 1.2 | 1.2 | 2 | 3 | 2.7 | 0.7 |
| 6-7 | 55.2 | 50.6 | 60.2 | 71 | 61.4 | 50.2 |
| 7-8 | 191 | 172.9 | 180.6 | 205.6 | 198.3 | 208.9 |
| 8-9 | 313.7 | 290.8 | 284.5 | 346.4 | 356.3 | 378.8 |
| 9-10 | 399.7 | 387.8 | 399.5 | 457.6 | 458.6 | 504.3 |
| 10-11 | 476.8 | 467 | 460.2 | 501.8 | 519.1 | 545.5 |
| 11-12 | 520.6 | 491.4 | 489.4 | 458 | 488.2 | 533.5 |
| 12-13 | 544.6 | 494.3 | 481.1 | 442.4 | 414.1 | 491.1 |
| 13-14 | 499.4 | 457.5 | 432.5 | 393.3 | 355.3 | 423.4 |
| 14-15 | 404.2 | 392 | 398.2 | 315.9 | 274.7 | 348.9 |
| 15-16 | 292.9 | 305.2 | 298.4 | 209.9 | 188.3 | 254.7 |
| 16-17 | 177.2 | 168.1 | 168.4 | 111 | 90.2 | 124.9 |
| 17-18 | 59.4 | 48.9 | 34.5 | 16.7 | 13 | 26 |
| 18-19 | 1.1 | 0.9 | 0.4 | 0.3 | 0.4 | 0.4 |
| 19-20 | 0.2 | 0.3 | 0.2 | 0.3 | 0.3 | 0.2 |
| 20-21 | 0.2 | 0.2 | 0.2 | 0.1 | 0.3 | 0.3 |
| 21-22 | 0.2 | 0.3 | 0.4 | 0.2 | 0.3 | 0.2 |
| 22-23 | 0.2 | 0.4 | 0.3 | 0.2 | 0.2 | 0.3 |
| 23-0 | 0.3 | 0.3 | 0.5 | 0.2 | 0.3 | 0.2 |
| Accumulated daily | 3939.9 | 3732.3 | 3693.8 | 3534.9 | 3423.7 | 3894.1 |

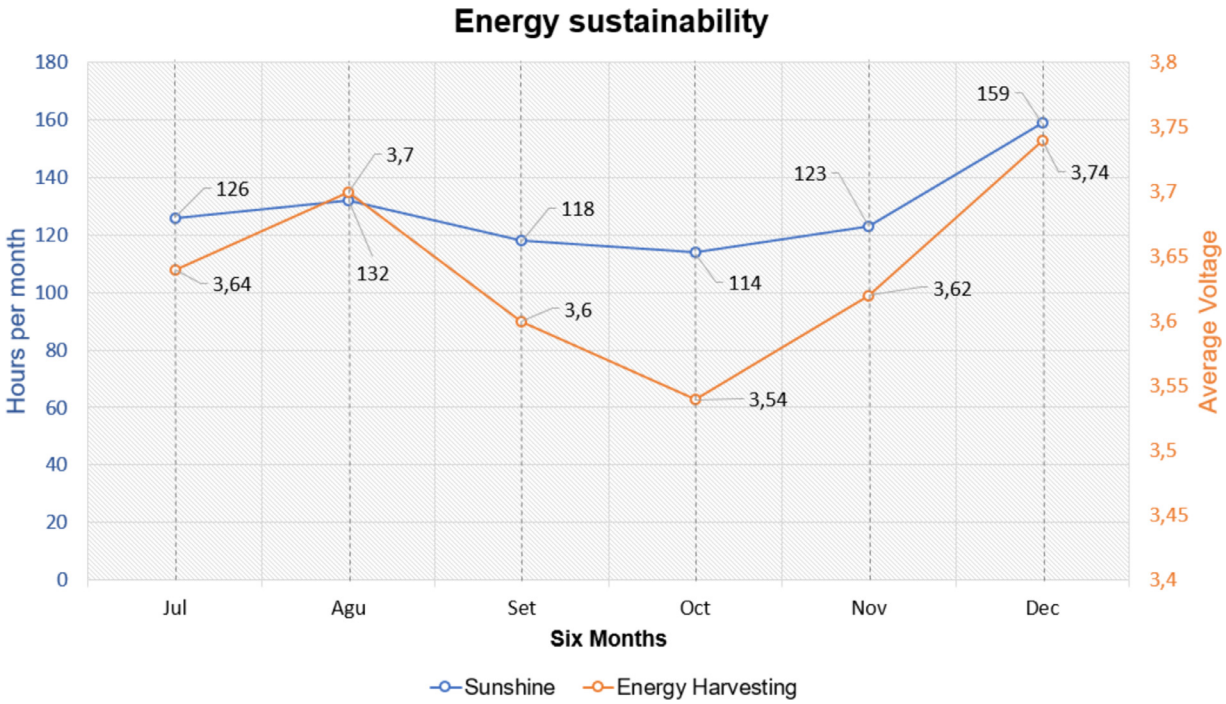


**Fig. 11.** Energy sustainability of the solar energy harvesting system during the months of july to december.

Table 10 shows that the highest correlation value between sunshine and voltage produced by the panel is 0.90855, indicating that the voltage produced by the solar panel depends on the sunshine value. The correlation value of 0.58580 between sunshine and solar irradiation, and of 0.61070 between voltage and irradiation, allow us to determine that variables such as rainfall and cloudiness suggest reciprocity between these variables, produced as an effect of condensation in cumulus clouds associated with weather conditions, which affect the availability of sunshine in the proposed energy collection system.

**Table 8**
Average value records for irradiation, sunshine, and voltage produced by the solar panel.

| Months | Sunshine | Energy Harvesting | Average Radiation ($W/m^2$) |
|---|---|---|---|
| July | 126 | 3.64 | 327.89166 |
| August | 132 | 3.7 | 310.54166 |
| September | 118 | 3.6 | 307.29166 |
| October | 114 | 3.54 | 294.13333 |
| November | 123 | 3.62 | 284.79166 |
| December | 159 | 3.74 | 324.18333 |
| Average | 128.66666 | 3.64 | 308.13888 |
| Variance | 216.55555 | 0.00426 | 232.55598 |

**Table 9**
Covariance matrix.

| | Sunshine | Energy harvesting | Average radiación ($W/m^2$) |
|---|---|---|---|
| Sunshine | 216.55555 | | |
| Energy harvesting | 0.87333 | 0.00426 | |
| Average radiación ($W/m^2$) | 131.46157 | 0.60833 | 232.55598 |

**Table 10**
Correlation matrix.

| | Sunshine | Energy harvesting | Average radiación ($W/m^2$) |
|---|---|---|---|
| Sunshine | 1 | | |
| Energy harvesting | 0.90855 | 1 | |
| Average radiación ($W/m^2$) | 0.58580 | 0.61070 | 1 |

## 6. Conclusions

The energy collection system proposed is sustainable, as it is able to power itself without any alternative power connections, maintaining efficiency by using NiMH batteries as a resource.

NiMH batteries provided energy for a time of 0.76 days (equivalent to 18.2 h) of node activity without the solar panel, in active mode. By activating sleep mode for a 37.5% work cycle, without a solar panel, the batteries were capable of providing energy for 2 days, extending the node life span by using sleep mode and performing the same work by alternating active and sleep modes. The estimated battery charge time was 1.077 days (equivalent to 55.848 h.) As the daylight time is of about 12 h, the solar power collection system was unable to fully charge the batteries in a single day, reaching a full charge in approximately 35 h. After two days, the system stabilizes itself and reaches energy autonomy, making the network node self-sustainable.

The work cycle configuration in sleep mode proposed in this article is ideal for applications that require monitoring up to 8 variables in a 30-second sampling interval, which was denominated a single time slot. The proposed energy collection system is not sustainable for data streaming applications, which leaves this option for future research. Possible applications for this system include monitoring environmental values in indoor spaces such as agriculture, gardening, home automation, and others.

Although the interpretation of the results of the covariance matrix is similar to the interpretation of the results of the correlation matrix for the variables of irradiation, sunshine, and voltage, they differ in the standardization of the coefficients of correlation by linear relationship, as seen between sunshine and panel voltage. The correlation value of 0.90855 is close to 1, thus indicating that the relationship is stronger than the relationships between voltage and irradiation, and irradiation and sunshine. The covariance values found were positive, which indicates a proportional dependence. The results of both the covariance and correlation matrices did not indicate that the proposed energy collection system is unsustainable.

The system presents a good level of functioning for integration into data storage and visualization platforms such as ThingSpeak, by integrating a low-cost system with the use of a generic solar panel, for which a direct proportion was found between solar brightness and voltage delivered by the solar panel.

## Declaration of interests

The authors declare that they have no known competing financial interests or personal relationships that could have appeared to influence the work reported in this paper.

## Acknowledgments

This work has been partly supported by the program of mobility of researchers in doctoral programs (DIE-UD-engineering) of the Distrital Francisco José de Caldas University, and under the support by the resolution 0124 of 26 November 2009 of the Fundación Universitaria los Libertadores.

## References

[1] E.G. Petrakis, S. Sotiriadis, T. Soultanopoulos, P.T. Renta, R. Buyya, N. Bessis, Internet of things as a service (iTaaS): challenges and solutions for management of sensor data on the cloud and the fog, Internet Things 3–4 (2018) 156–174, doi:10.1016/j.iot.2018.09.009.
[2] P. Asghari, A.M. Rahmani, H.H.S. Javadi, Internet of things applications: a systematic review, Comput. Netw. 148 (2019) 241–261, doi:10.1016/j.comnet.2018.12.008.
[3] L. Muduli, D.P. Mishra, P.K. Jana, Application of wireless sensor network for environmental monitoring in underground coal mines: a systematic review, J. Netw. Comput. Appl. 106 (2018) 48–67, doi:10.1016/j.jnca.2017.12.022.
[4] P. Kaur, B.S. Sohi, P. Singh, Recent advances in MAC protocols for the energy harvesting based WSN: a comprehensive review, Wirel. Person. Commun. 104 (1) (2019) 423–440, doi:10.1007/s11277-018-6028-3.
[5] S. Ulukus, A. Yener, E. Erkip, O. Simeone, M. Zorzi, P. Grover, K. Huang, Energy harvesting wireless communications: a review of recent advances, IEEE J. Sel. Areas Commun. 33 (3) (2015) 360–381, doi:10.1109/JSAC.2015.2391531.
[6] G. Han, L. Liu, J. Jiang, L. Shu, G. Hancke, Analysis of energy-efficient connected target coverage algorithms for industrial wireless sensor networks, IEEE Trans. Ind. Inform. 13 (1) (2017) 135–143, doi:10.1109/TII.2015.2513767.
[7] C. Lu, A. Saifullah, B. Li, M. Sha, H. Gonzalez, D. Gunatilaka, C. Wu, L. Nie, Y. Chen, Real-time wireless sensor-actuator networks for industrial cyber-physical systems, Proc. IEEE 104 (5) (2016) 1013–1024, doi:10.1109/JPROC.2015.2497161.
[8] Y. Wang, H. Chen, X. Wu, L. Shu, An energy-efficient SDN based sleep scheduling algorithm for WSNS, J. Netw. Comput. Appl. 59 (2016) 39–45, doi:10.1016/j.jnca.2015.05.002.
[9] T.N. Le, A. Pegatoquet, T. Le Huy, L. Lizzi, F. Ferrero, Improving energy efficiency of mobile WSN using reconfigurable directional antennas, IEEE Commun. Lett. 20 (6) (2016) 1243–1246, doi:10.1109/LCOMM.2016.2554544.
[10] Research BCC, Global markets, technologies and devices for energy harvesting, 2018, Accessed: 2019-04-19 URL https://www.bccresearch.com/market-research/energy-and-resources/global-markets-technologies-and-devices-for-energy-harvesting.html.
[11] D. Bruneo, S. Distefano, M. Giacobbe, A.L. Minnolo, F. Longo, G. Merlino, D. Mulfari, A. Panarello, G. Patané, A. Puliafito, C. Puliafito, N. Tapas, An IoT service ecosystem for smart cities: the #smartme project, Internet Things 5 (2019) 12–33, doi:10.1016/j.iot.2018.11.004.
[12] A. Somov, Z.J. Chew, T. Ruan, Q. Li, M. Zhu, Poster abstract: piezoelectric energy harvesting powered WSN for aircraft structural health monitoring, in: Proceedings of the Fifteenth ACM/IEEE International Conference on Information Processing in Sensor Networks (IPSN), 2016, pp. 1–2, doi:10.1109/IPSN.2016.7460711.
[13] S. Baghaee, H. Ulusan, S. Chamanian, O. Zorlu, H. Kulah, E. Uysal-Biyikoglu, Towards a vibration energy harvesting WSN demonstration testbed, in: Proceedings of the Twenty Fourth Tyrrhenian International Workshop on Digital Communications–Green ICT (TIWDC), 2013, pp. 1–6, doi:10.1109/TIWDC.2013.6664202.
[14] L. Hou, S. Tan, Z. Zhang, N.W. Bergmann, Thermal energy harvesting WSNs node for temperature monitoring in IIoT, IEEE Access 6 (2018) 35243–35249, doi:10.1109/ACCESS.2018.2851203.
[15] G. Verma, V. Sharma, A survey on hardware design issues in RF energy harvesting for wireless sensor networks (WSN), in: Proceedings of the Fifth International Conference on Wireless Networks and Embedded Systems (WECON), 2016, pp. 1–9, doi:10.1109/WECON.2016.7993469.
[16] R. Ibrahim, T.D. Chung, S.M. Hassan, K. Bingi, S.K. binti Salahuddin, Solar energy harvester for industrial wireless sensor nodes, Procedia Comput. Sci. 105 (2017) 111–118. 2016 IEEE International Symposium on Robotics and Intelligent Sensors, IRIS 2016, 17–20 December 2016, Tokyo, Japan. doi:10.1016/j.procs.2017.01.184.
[17] S. Cao, J. Li, A survey on ambient energy sources and harvesting methods for structural health monitoring applications, Adv. Mech. Eng. 9 (4) (2017. ), doi:10.1177/1687814017696210.
[18] M. Das, D. Mukherjee, A standalone charging station for li-ion digital camera battery from solar photovoltaic module with supercapacitor, in: Proceedings of the Third International Conference on Computer, Communication, Control and Information Technology (C3IT), 2015, pp. 1–3, doi:10.1109/C3IT.2015.7060213.
[19] A. González, E. Goikolea, J.A. Barrena, R. Mysyk, Review on supercapacitors: technologies and materials, Renew. Sustain. Energy Rev. 58 (2016) 1189–1206, doi:10.1016/j.rser.2015.12.249.
[20] S. Senivasan, M. Drieberg, B.S.M. Singh, P. Sebastian, L.H. Hiung, An MPPT micro solar energy harvester for wireless sensor networks, in: Proceedings of the IEEE Thirteenth International Colloquium on Signal Processing its Applications (CSPA), 2017, pp. 159–163, doi:10.1109/CSPA.2017.8064943.
[21] J. Taneja, J. Jeong, D. Culler, Design, modeling, and capacity planning for micro-solar power sensor networks, in: Proceedings of the Seventh International Conference on Information Processing in Sensor Networks, in: IPSN '08, IEEE Computer Society, Washington, DC, USA, 2008, pp. 407–418, doi:10.1109/IPSN.2008.67.
[22] P. Srivastava, M. Bajaj, A.S. Rana, IoT based controlling of hybrid energy system using esp8266, in: Proceedings of the IEEMA Engineer Infinite Conference (eTechNxT), 2018, pp. 1–5, doi:10.1109/ETECHNXT.2018.8385294.
[23] P. Jariyayothin, K. Jeravong-aram, N. Ratanachaijaroen, T. Tantidham, P. Intakot, IoT backyard: smart watering control system, in: Proceedings of the Seventh ICT International Student Project Conference (ICT-ISPC), 2018, pp. 1–6, doi:10.1109/ICT-ISPC.2018.8523856.
[24] AccuWeather, Inc., Colombia Weather-Local Weather, URL https://www.accuweather.com/en/co/colombia-weather.
[25] IDEAM and UPME., Atlas de radiación solar, ultravioleta y ozono de colombia, URL http://atlas.ideam.gov.co/visorAtlasRadiacion.html.